

# The Regional Intraplate Stress Field in South America

MARCELO ASSUMPCAO

*Departamento de Geofísica, Instituto Astronômico e Geofísico, Universidade de São Paulo, Brazil*

A compilation of lithospheric stress directions for continental South America and the inferred major patterns of the regional intraplate stress field are presented. Stress orientations are based primarily on earthquake focal mechanisms and Quaternary fault slip inversion published in the literature. Four new focal mechanisms based on short-period  $P$  wave modeling, and selected centroid-moment-tensor solutions (published by U.S. Geological Survey) consistent with  $P$  wave first motions at South American and other World-Wide Standard Seismograph Network stations are also included in the data base. The observed patterns of intraplate stresses may be useful in constraining numerical models of the plate driving forces in the South American plate. In the Andean plateau (altitudes greater than 3000 m), N-S extensional stresses predominate. E-W compressional stresses are observed in the sub-Andean and platform regions extending up to about 1000 km east of the Andes. The maximum horizontal stress ( $SH_{max}$ ) is uniformly oriented in the E-W direction throughout western South America. Averages of the  $SH_{max}$  direction at grid points spaced  $2.5^\circ$  were taken as representing the "regional" field. The E-W direction of this regional field is not affected by the change of strike of the Andean chain nor by the contact of a flat subducted slab underneath. The regional  $SH_{max}$  direction is oriented  $15^\circ$  more clockwise than the direction of the Nazca plate convergence. The difference between the regional  $SH_{max}$  orientations and the absolute plate motion may be only about  $6^\circ$ . This may indicate that contact forces with the Nazca plate may not be the only major contributor to the intraplate stresses in western South America. The eastern limit of this Andean stress province seems to coincide with aseismic regions in the Upper Amazon basin and in the Paraná basin. In the central Amazonian region, seismicity and stress data suggest a seismic province with N-S compressional stresses. The origin of these stresses is not yet clearly understood but could possibly be related to lower crustal loading along the middle Amazon basin. In northeastern Brazil, seismicity is characterized by upper crustal strike-slip earthquakes bordering the Potiguar marginal basin. A model is proposed for this region in which the stress field is the result of a superposition of regional E-W compressional stresses and local extensional stresses (oriented perpendicular to the continental margin) possibly related to density contrasts and sediment loading in the continental shelf.

## INTRODUCTION

The state of stress in the lithosphere can be due to both local forces (e.g., stress concentrations due to structure heterogeneities, crustal loading and unloading, asthenospheric thermal anomalies) and regional, more uniform forces directly related to plate motion (such as ridge-push, negative buoyancy of the subducted slab, and viscous shear forces in the asthenosphere-lithosphere boundary). The tectonic setting of South America is unique: In no other part of the world does a major oceanic plate subduct beneath a large continental plate along a trench almost 6000 km long. Due to the large extent and relatively uniform Andean tectonism (compared with other subduction zones) the regional stress field in continental South America could be expected to be more uniform than in other smaller overriding plates where lithospheric heterogeneities, such as in island arcs, may mask the effect of plate driving forces. For this reason the regional lithospheric stresses in the continental part of the overriding South American plate may be useful for inferring the relative importance of some of the driving forces that cause plate motions.

In western South America, shallow earthquakes in the upper plate usually have thrusting mechanisms with  $P$  axes roughly in the E-W direction, approximately parallel to the direction of the Nazca plate subduction. For this reason, since the pioneering work of Stauder [1973, 1975], it has been common to attribute any compressional stresses as being caused by the Nazca-South America plate "collision" [Suárez *et al.*, 1983; Chinn and Isacks, 1983; Assumpção and Suárez, 1988]. A horizontal compression due to the convergence of the Nazca plate has also

been used, coupled with the gravitational effect of the Andean topography, to explain the N-S extensional normal stresses observed in the high Andes of Peru and Bolivia [Sebrier *et al.*, 1985, 1988; Mercier *et al.*, this issue]. The Nazca plate "collision" has seemed a natural explanation for any horizontal compression in western South America even though other forces, such as those in the lithosphere-asthenosphere boundary, could also be considered because the absolute plate motion is approximately E-W. In fact, Zoback *et al.* [1989] have shown that the maximum horizontal stress ( $SH_{max}$ ) in South America tends to be roughly parallel to the absolute plate motion.

The small difference between the convergence and absolute motion directions in western South America (about  $10^\circ$ , usually less than the accuracy of any single stress determination) makes it difficult to separate their contribution to the intraplate stress field. Also, the prominent Andean tectonic features related to the Nazca plate subduction seem to have overshadowed the lithosphere-asthenosphere boundary forces as potential contributors to plate stresses. The amount of stress data compiled as part of the World Stress Map Project may begin to reveal the importance of other sources of stress in South America.

In central and eastern South America, few stress data are available. Due to the low midplate seismicity and low density of seismographic stations, focal mechanisms could be determined for only a few events with magnitudes about  $m_b$  5 occurred in the last decades. The first focal mechanisms determined in midplate South America by Mendiguren and Richter [1978] were consistent with a uniform compressional stress field oriented roughly NW-SE. However, the presently available data, although not yet enough for a complete definition of the midplate stress patterns, do show that the stress field is not uniform, suggesting that local sources are important compared with regional forces.

Copyright 1992 by the American Geophysical Union.

Paper number 91JB01590.  
0148-0227/92/91JB-01590\$05.00

## STRESS DATA BASE FOR SOUTH AMERICA

The intraplate stress data for South America (Figure 1) come mainly from earthquake focal mechanisms (43%) and geological data (50%). Few breakout and in situ measurements are available in this region. Figure 1 shows the directions of the maximum horizontal stress ( $SH_{max}$ ) throughout South America. This single stress axis is plotted to facilitate definition of regional stress patterns;  $SH_{max}$  corresponds to the maximum principal stress direction for thrust and strike-slip tectonic regimes and to the intermediate principal stress direction for normal faulting regimes ( $B$  axes of the focal mechanism solutions).

*Earthquake Focal Mechanisms*

The focal mechanism solution of a single earthquake does not give directly the orientation of the principal stresses acting in the lithosphere, but only the directions of that part of the stress released by the earthquake [McKenzie, 1969]. However, experience has shown that the differences between the orientations of the  $P$  and  $T$  axes of the focal mechanism solution and the principal directions of the stress field are not usually more than about  $30^\circ$  [e.g., Raleigh et al., 1972]. Also, in areas under compression, the average of  $P$  directions of various independent earthquakes tend to be close to the  $S_1$  direction (maximum principal compression) of the regional stress field [Zoback and Zoback, 1980; Zoback, this issue (b)].

Focal mechanism data for South American intraplate earthquakes come from three sources: (1) previously published mechanisms compiled from the literature, (2) four new solutions presented below, and (3) Harvard centroid-moment-tensor solutions checked against  $P$  wave polarities. The compilation of published data did not include events near the Pacific coast which, depending on their focal depth, could be associated directly with slip between the Nazca and South American plates in the subduction zone. Few studies of intraplate earthquakes have been published for South America. Stauder [1973] determined focal mechanisms of 61 Andean events near the central and northern Chile subduction zone, but only one earthquake was a shallow intraplate event. In another study of the subduction of the Nazca plate beneath Peru and Ecuador, Stauder [1975] determined 40 focal mechanisms, 10 of which were shallow intraplate. Suárez et al. [1983] reexamined these 10 events and included seven other focal mechanisms in a study of intraplate tectonics in Peru, Ecuador, and southern Colombia. Chinn and Isacks [1983] determined source depths and focal mechanisms of 28 shallow intraplate earthquakes from Ecuador to Argentina; their data set included the same intraplate events studied by Stauder [1973, 1975]. In western South America, additional intraplate focal mechanisms were determined for shallow events in Peru [Grange et al., 1984; Dorbath et al., 1986; Carey-Gailhardis and Mercier, 1987; Doser, 1987; Deverchere et al., 1989] and for the San Juan (Caucete, Argentina) 1977 earthquakes [Kadinsky-Cade and Reilinger, 1985]. Focal mechanisms of 10 shallow (mostly strike-slip) events in Colombia and Venezuela near the Caribbean plate [Pennington, 1981; Kafka and Weidner, 1981] were also included because of the diffuse nature of the plate boundary in that region characterized by a broad zone of internal deformation. East of the Andean region, Mendiguren and Richter [1978], Assumpção et al. [1985], and Assumpção and Suárez [1988] determined focal mechanisms of 11 midplate events in Brazil. Studies of a dam-induced activity in southeastern Brazil [Mendiguren, 1980] and some earthquake swarms in northeastern Brazil [Ferreira et al.,

1987, 1989; Sophia and Assumpção, 1989; Assumpção et al., 1989, 1990] have provided mechanisms of some events along the South Atlantic coast.

All focal mechanisms have been examined and classified into three quality categories (B, C, and D) according to the reliability of the estimate of the maximum horizontal stress,  $SH_{max}$ , [Zoback, this issue (a)]. In terms of the  $P$  and  $T$  directions of the earthquake focal mechanism, the three classes roughly correspond to uncertainties of  $\pm 5^\circ$ (B),  $\pm 20^\circ$ (C) and  $\pm 40^\circ$ (D). The highest quality A was only used for stress tensor inversion using several independent focal mechanisms in the same area.

Figure 2 and Table 1 show four new focal mechanisms of intraplate events (one near the Peru-Brazil border, one in Argentina, one in Paraguay, and one near the Chile-Argentina border) determined by modeling the relative amplitudes of the short-period depth phases  $pP$  and  $sP$ , as described by Assumpção and Suárez [1988]. All mechanisms are reverse faulting with roughly E-W oriented  $P$  axes. These four mechanisms, despite the good fit of the  $pP$  and  $sP$  amplitudes, have been classified as quality C because of the uncertainties of the  $P$  axis direction.

*Harvard Centroid-Moment-Tensor Solutions*

In order to increase the data base for South America, centroid-moment-tensor solutions (CMT), determined by Harvard [Dziewonski and Woodhouse, 1983] and published in the U.S. Geological Survey's Earthquake Data Report, were also examined. The CMT solution is the result of simultaneous inversion of long-period waveform data to obtain the hypocentral parameters (epicenter, depth, and origin time) and the elements of the seismic moment tensor of the best point source. Body waves with periods greater than 45 s are generally used. For moderate size earthquakes ( $m_b$  5 to 6) CMT inversions can give results which are quite different from the "correct" nodal plane solutions. For example, Assumpção and Suárez [1988] determined a reverse fault focal mechanism for a 23-km-deep event in the Amazon basin using a good distribution of  $P$  wave polarities together with  $P$  wave modeling and found  $80^\circ$  difference in the  $P$  azimuth between their mechanism and the CMT solution (which was also a reverse fault mechanism). This was probably due to the instability of CMT inversion for shallow dip-slip earthquakes [Sipkin, 1986; Anderson, 1988]. For this reason, although CMT inversions are valuable for global statistical studies and provide a good indication of the general style of deformation in an area, careful consideration of first motion data is still necessary for detailed study of source mechanics and regional tectonics [Anderson, 1988].

Thirty-nine CMT solutions for intraplate events, from January 1982 to June 1990, were checked for consistency with  $P$  wave polarities at World-Wide Standard Seismograph Network stations and some high-gain Brazilian stations. From this comparison, two solutions were found to be wrong (i.e., the CMT seemed incompatible with the polarity data) and 14 CMT solutions were found to be uncertain (the quality and number of polarities were not enough to be used as a check of the CMT solutions). The other 23 events were found to have CMT solutions in general agreement with the  $P$  wave polarities and were included in the data base with quality C (see Figure 3 and Table 2). The two events with inconsistent  $P$  wave first motions are shown in Figure 4. The event 870306C ( $m_b$  5.5) was an aftershock of the  $m_b$  6.5 Colombia earthquake occurred on the same day: the polarity data indicate that the mechanism of the

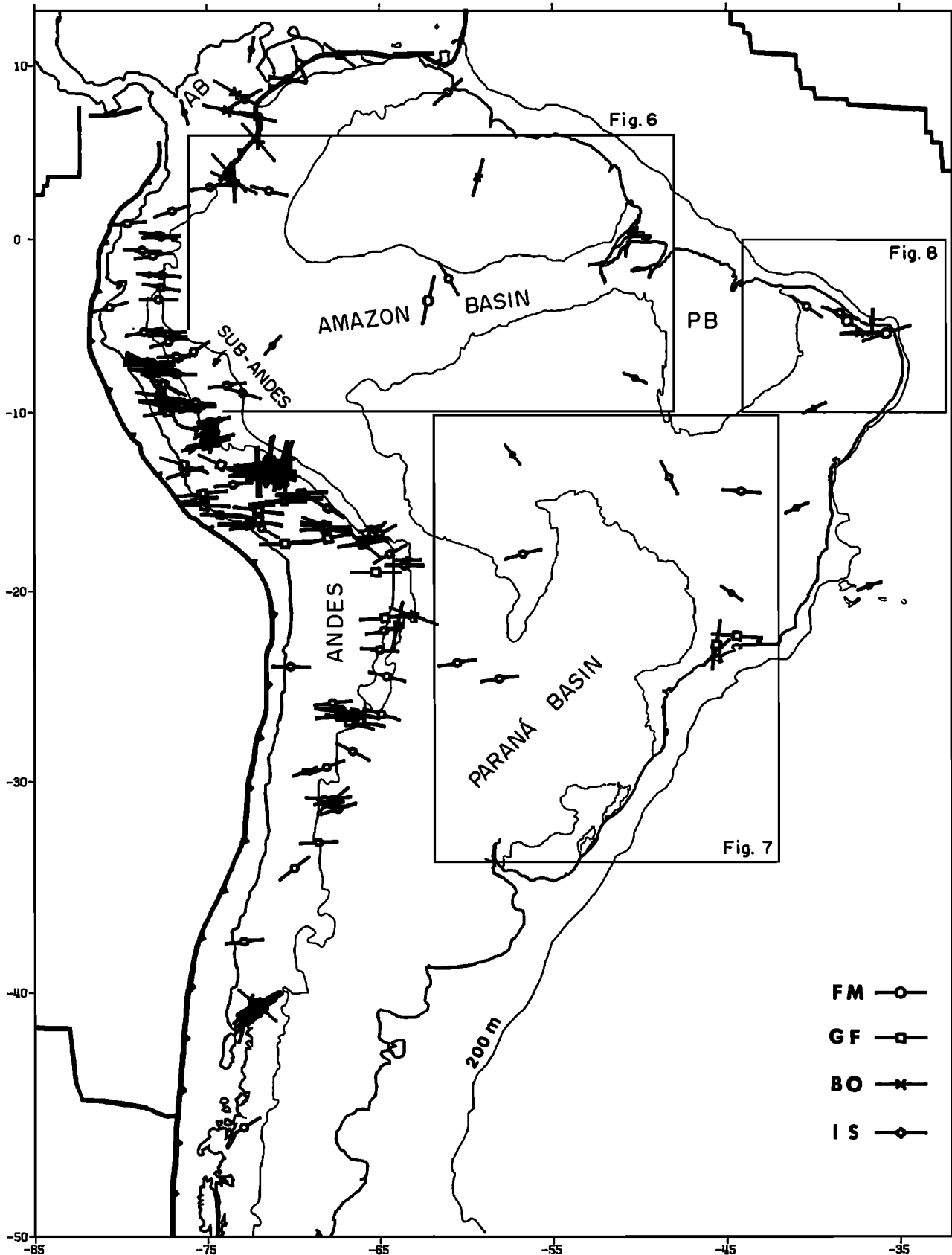


Fig. 1. Maximum horizontal stress ( $SH_{max}$ ) orientations in South America. Large symbols corresponds to data quality 'A' and 'B'; intermediate size to quality 'C'; small size to quality 'D'. Only the boundaries between the major geotectonic units (Andean chain, sub-Andean foredeep and platforms) are shown together with the main, deep intracratonic basins [Departamento Nacional de Produção Mineral, 1978]. PB is Paraíba basin. Saw-toothed lines mark the axis of the Peru-Chile trench and the eastern Andean frontal fault zone [Pennington, 1981] which delimits the Andean block (AB) in Colombia and Venezuela. The stress data are derived from focal mechanisms (FM), geological faults (GF), breakouts (BO), and in situ measurements (IS).

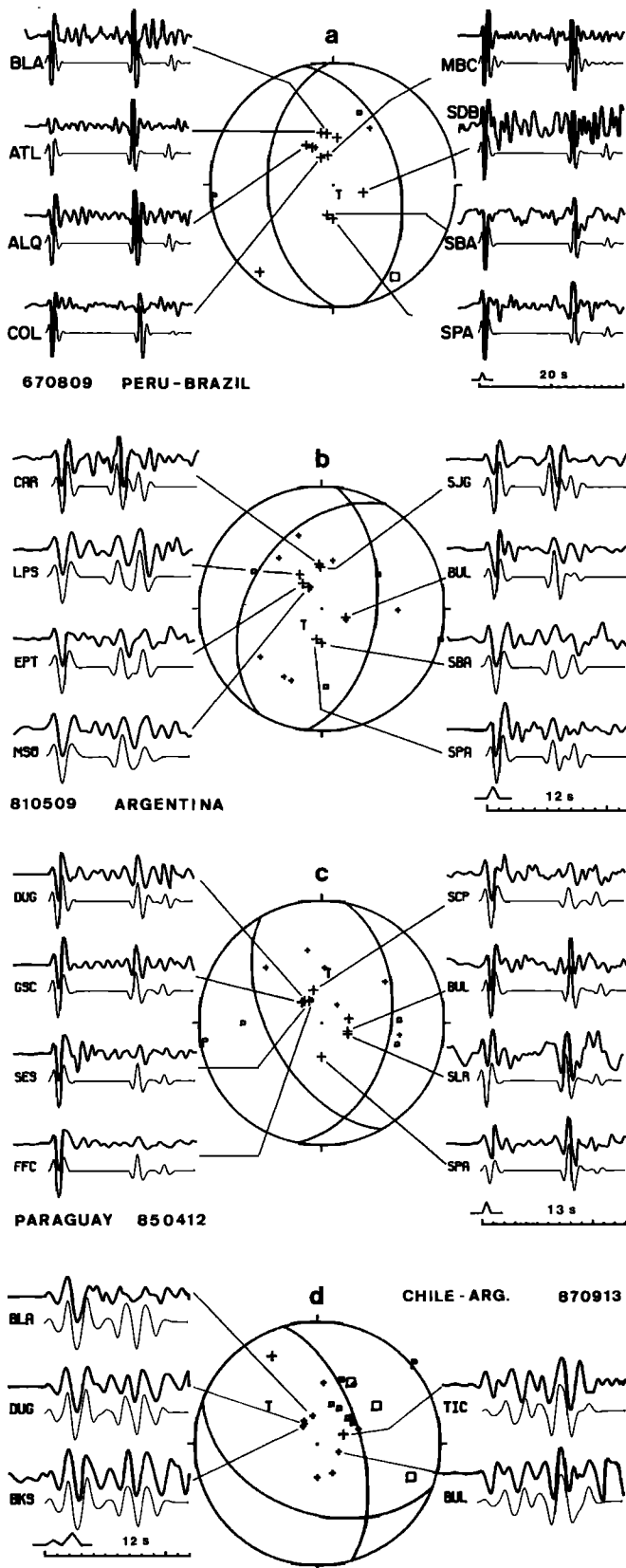


Fig. 2. Additional focal mechanism solutions of intraplate earthquakes (Table 1) obtained by modeling the amplitudes of the  $P$ ,  $pP$ , and  $sP$  phases. Upper and lower traces are observed and synthetic seismograms, respectively. In the equal-area projection, large and small symbols denote more and less reliable polarities. Crosses and squares are compressional and dilatational  $P$  wave first motions, respectively. The signal near the beginning of the time scale represents the source time function. Numbers are event date (year, month, day).

aftershock was not much different from that of the main event (dip-slip, shallow, reverse fault, as shown in Figure 3 and Table 2). The polarity data for the event 870913 indicate that the NE striking nodal plane (Figure 4b) is not correct. Two alternatives are possible: a strike-slip solution with vertical nodal planes or a predominantly reverse faulting with one nodal plane striking about N-S and steeply dipping to the east. An examination of the amplitudes of the depth phases  $pP$  and  $sP$  favors the dip-slip alternative as presented in Figure 2d (the polarity misfits correspond to less reliable data near one of the nodal planes). Thus the two events with inconsistent CMT solutions had shallow dip-slip mechanisms.

#### Geological Data

In the Peruvian and Bolivian Andes, a large research program to analyze Quaternary and recent faults has been under way for many years [Mercier, 1981; Sebrier *et al.*, 1985, 1988; Cabrera *et al.*, 1987; Bellier *et al.*, 1989; Bonnot *et al.*, 1988; Mercier *et al.*, this issue] with stress directions determined at about 40 sites covering many different fault systems. Thus the majority of the geological data in Figure 1 are from Peru and Bolivia. In the Puna plateau of northwestern Argentina (just south of the sub-Andean province in Figure 1), Allmendinger *et al.* [1989] have determined stress directions from Quaternary fault slip data in five different sites. Data sets from both Peru-Bolivia and NW Argentina show that normal faulting predominates in the high Andes, whereas thrust faults tend to occur in the sub-Andean and Precordillera regions, a pattern also observed in the earthquake data.

Stress directions have also been inferred from sets of fault striae at some Pleistocene faults in southeastern Brazil [Riccomini *et al.*, 1989] and alignment of volcanic vents in southern Chile [Katsui and Katz, 1967; Roa, 1976].

#### Breakout Measurements

The maximum horizontal stress directions ( $SH_{max}$ ) can be determined from tectonic elongations observed in deep boreholes [e.g., Bell and Gough, 1979; Cox, 1983; Zoback *et al.*, 1985]. These elongations are caused by shear fractures of the borehole wall ("breakouts") due to a redistribution of the stresses around the hole; these stress-induced breakouts are observed on opposite sides of the borehole wall in the direction of the minimum horizontal stress [Zoback *et al.*, 1985]. Other borehole elongations caused by the drilling process which are not related to the crustal stresses can be distinguished from the tectonic breakouts through careful analysis of the borehole logs [Cox, 1983; Plumb and Hickman, 1985].

Breakouts have been increasingly used to estimate the crustal stress directions [e.g., Zoback and Zoback, 1989; Zoback *et al.*, 1989]. Unfortunately, few breakout measurements are available in South America. Breakouts from five oil wells in Colombia [Castillo and Mojica, 1989] in the region of the Caribbean-South American plate boundary (Figure 1) are generally consistent with focal mechanism data. Cox [1983] published breakout orientations for two wells in the Bolivian sub-Andes and one in Guyana. In northeastern Brazil, two breakouts (C. Lima, written communication, 1990) ranked with qualities C and D, complement the focal mechanism data.

#### In Situ Stress Measurements

Only two direct measurements of stress have been compiled, one hydraulic fracturing in central Brazil and an overcoring in northeastern Brazil (Figure 1). In central Brazil, measurements

TABLE 1. Focal Mechanism Parameters of the Earthquakes in Figure 2

Date	Time UT	Latitude deg	Longitude deg	Depth km	$m_b$	Azimuth/Plunge, deg		Region
						P Axis	T Axis	
Aug. 9, 1967	0714:08	-8.45	-73.83	42	5.1	262/00	169/84	Peru-Brazil
May 9, 1981	0950:40	-26.57	-64.90	15	5.0	108/07	227/76	Argentina
April 12, 1985	1434:57	-23.94	-60.55	21	5.3	259/06	4/68	Paraguay
Sept. 13, 1987	2008:52	-34.33	-69.97	13	5.8	51/10	303/60	Chile-Argentina

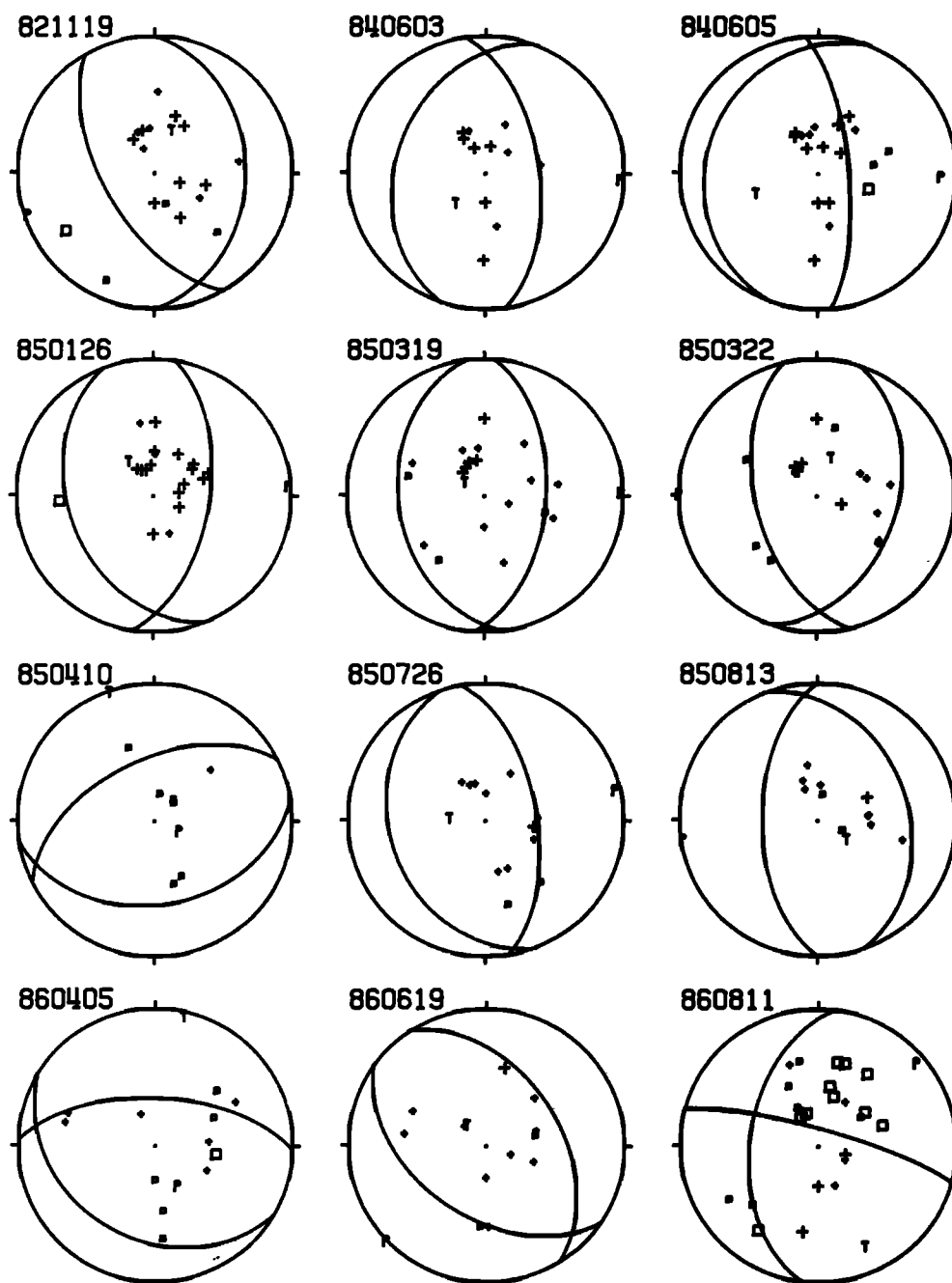


Fig. 3. Harvard centroid-moment-tensor solutions (best double couple) consistent with polarity data as recorded by WWSSN and South American stations. Crosses and squares are compressional and dilatational first motions; smaller symbols denote less reliable polarity data. Identification numbers are the earthquake dates as shown in Table 2.

with hydraulic fracturing were made in two nearby shallow wells (100 and 150 m deep) drilled in granite for engineering studies at a dam site [Caproni and Armelin, 1990]. The average NW-SE direction of the two orientations (with 25° difference) was given a C quality because of the shallow depth sampled; no

information was available on local topography at the site.  $SH_{max}$  is greater than the lithostatic pressure, implying a compressional state of stress in that area. In northeastern Brazil, several overcoring measurements were made in an underground mine at depths ranging from 280 to 490 m [Cipriani, 1990]. The result-

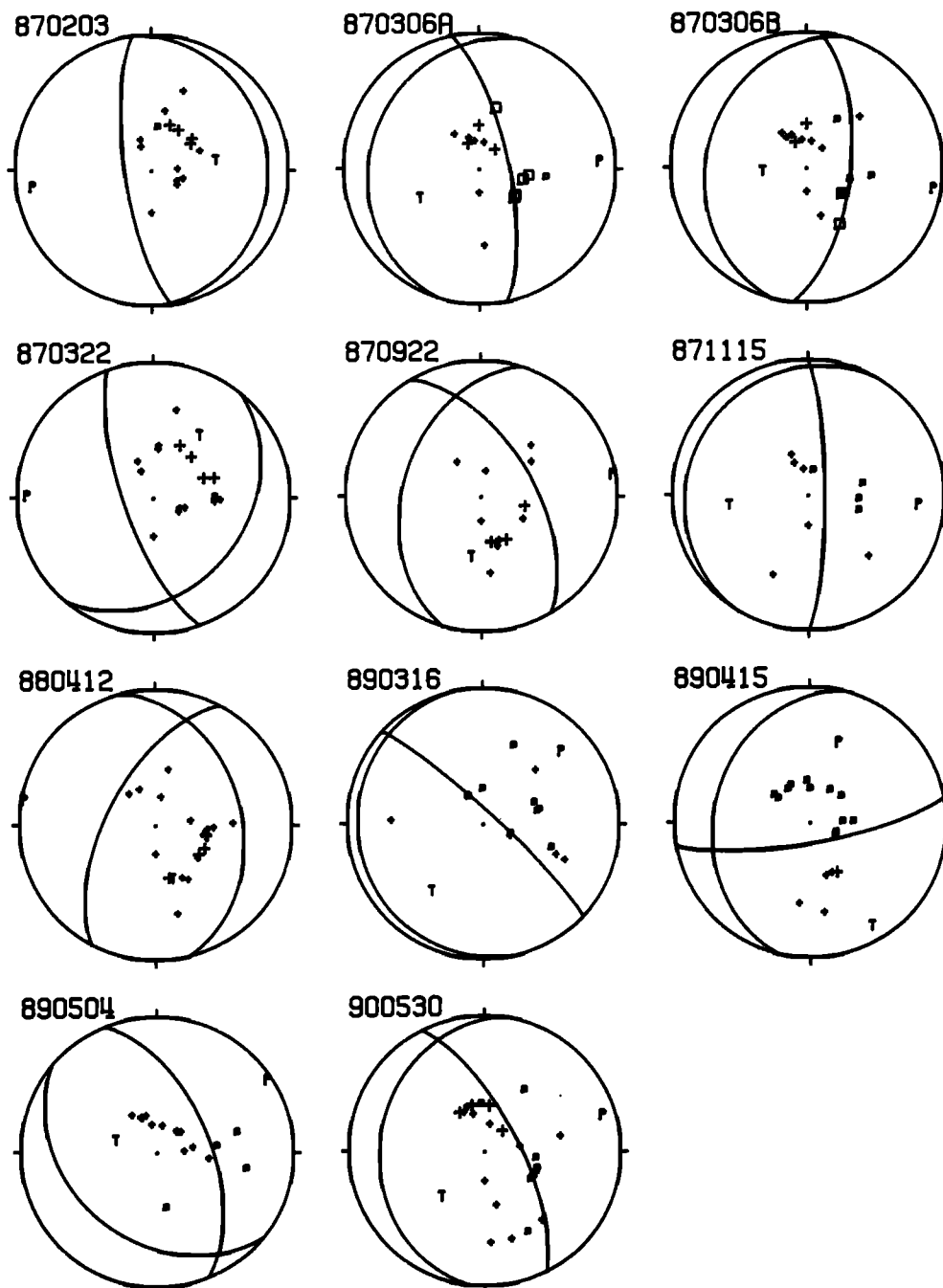


Fig. 3 (cont.).

ing magnitudes and orientations had large uncertainties and were very scattered; the five best results (with magnitude errors less than 40%) gave an average azimuth for  $SH_{max}$  of  $N64^{\circ}E$  ( $\pm 27^{\circ}$ ). This was given a D quality.

#### STATE OF STRESS IN THE ANDEAN REGION

##### Northwestern South America

The southern limit of the Caribbean plate in the region of Panama, Colombia, and Venezuela is characterized by a broad zone of internal deformation [Pennington, 1981; Kafka and Weidner, 1981]. This zone is called "Andean block" and is indicated in Figure 1. Deformation is accommodated by mainly strike-slip motion on many different faults. Despite the few available stress data for a detailed description of the stress field,

an average E-W to SE-NW oriented  $SH_{max}$  seems to be present in the Andean block which would be consistent with the ESE motion of the Caribbean plate relative to the South American plate [DeMets *et al.*, 1990] as shown in Figure 6.

##### Stress Patterns in Western South America

Throughout the Andean region, from about  $3^{\circ}N$  to  $40^{\circ}S$ ,  $SH_{max}$  is oriented predominantly E-W. The histograms of Figure 5a compare the  $SH_{max}$  orientations with the direction of the South America absolute plate motion, which is essentially E-W [Minster and Jordan, 1978]. The geological data generally cluster about the local absolute plate motion azimuth; however, the orientations show a secondary peak roughly oriented N-S corresponding to upper Pliocene-lower Pleistocene faults from

TABLE 2. Focal Mechanisms Determined by Harvard (Centroid-Moment-Tensor Solution as Published in the Earthquake Data Reports of the U.S. Geological Survey) Compatible with P Wave First Motion at South American and WWSSN Stations

Date	Time UT	Latitude deg	Longitude deg	Depth km	$m_b$	Azimuth/Plunge, deg		Region
						P Axis	T Axis	
Nov. 11, 1982	0427:14	-10.61	-74.69	14*	6.3	252/14	24/70	Peru
June 3, 1984	0410:27	-7.80	-76.78	34	5.3	92/12	224/72	Peru
June 5, 1984	0415:24	-7.82	-76.71	25	5.8	91/26	251/62	Peru
Jan. 26, 1985	0306:58	-33.07	-68.58	15*	5.8	86/09	325/72	Argentina
March 19, 1985	1028:36	-18.60	-63.58	19	5.4	89/07	307/81	Bolivia
March 22, 1985	1402:41	-18.63	-63.56	9	5.4	271/06	21/73	Bolivia
April 10, 1985	2015:37	+1.56	-77.02	10	5.3	113/79	342/07	Colombia
July 26, 1985	1756:58	-5.38	-78.65	18	5.3	77/14	274/75	Peru
Aug. 13, 1985	0529:19	-15.04	-75.47	25	5.4	262/11	124/76	Peru
April 5, 1985	2014:29	-13.41	-71.78	51	5.3	152/70	14/15	Peru
June 19, 1986	2157:24	-16.94	-65.43	20	5.4	226/01	320/79	Bolivia
Aug. 11, 1986	2206:43	-30.92	-67.68	25*	5.4	50/20	155/35	Argentina
Feb. 3, 1987	1642:41	-37.75	-72.89	32*	5.8	263/29	80/61	Chile
March 6, 1987A	0154:50	+0.05	-77.65	14	6.1	86/27	244/71	Colombia
March 6, 1987B	0410:42	+0.15	-77.82	10	6.5	100/19	268/71	Colombia
March 22, 1987	0323:58	-24.06	-70.14	40*	5.8	271/23	38/55	Chile
Sept. 22, 1987	1621:35	-1.08	-78.13	10	5.9	80/09	190/63	Ecuador
Nov. 15, 1987	2200:50	-9.43	-75.66	32	5.4	95/34	262/55	Peru
April 12, 1988	1526:20	-2.79	-77.65	27	5.5	281/12	162/66	Peru
March 16, 1989	1712:22	-16.93	-65.00	44	5.1	48/38	217/52	Bolivia
April 15, 1989	1426:41	+8.45	-61.04	23	5.8	20/51	149/28	Venezuela
May 4, 1989	1030:07	-6.61	-75.76	36	5.5	57/12	287/72	Peru
May 30, 1990	0234:06	-6.02	-77.23	24	6.1	73/24	223/63	Peru

See Figure 3.

\*Depth calculated with  $pP$  phases by the author or by U.S.G.S.

southern Peru (about 14°S in Figure 1). This may be due to a change of  $SH_{max}$  direction during the Quaternary [Bonnot *et al.*, 1988; Mercier *et al.*, this issue]. Figure 5b shows  $SH_{max}$  orientations in western South America from both focal mechanisms and recent geological data (i.e., excluding the upper Pliocene to lower Pleistocene data) separated into two classes: reverse and normal faulting regimes. In the high Andes (elevations greater than 3000 m), normal faulting tends to prevail with extension usually in the N-S direction (E-W  $SH_{max}$ ) which has been interpreted as due to the topographical load of the high Andes overcoming the regional E-W compression making S1 vertical and S2 E-W [Sebrier *et al.*, 1985, 1988; Froidevaux and Ricard, 1987; Mercier *et al.*, this issue]. Reverse faulting tends to occur at the lower altitudes in the sub-Andes. In Figure 5b the few focal mechanisms available in the high Andes reflect the lower seismicity of the Altiplano-Puna plateau [Suárez *et al.*, 1983].

In a high plateau such as in the Andes, extensional stresses may develop perpendicular to the axis of the plateau as a result of the combined effect of the high topography and the buoyance of the compensating crustal root [Fleitout and Froidevaux, 1982; Froidevaux and Ricard, 1987]. These stresses tend to cause normal faulting with  $SH_{max}$  parallel to the axis of the plateau. The resulting tectonic regime depends on the balance between these plateau-induced stresses and the compressional stresses due to the plate convergence. Bonnot *et al.* [1988] and Mercier *et al.* [this issue] have shown that this balance has varied since the Pliocene in the Andes of Peru and Bolivia. In the Pliocene, E-W to NE-SW extension occurred in the High Andes with the apparent dominance of the topographical effect over horizontal compression being interpreted as associated with a low convergence rate of the Nazca plate. In early Quaternary, major E-W compressional deformation (and also minor N-S trending compression) was observed in the whole Andes and interpreted as due to predominance of plate contact forces (high

convergence rate of the Nazca plate). From late Quaternary to present an intermediate situation results in N-S extension in the High Andes and E-W compression in the sub-Andes.

It is interesting to note in Figure 5a that the recent geological data have an average  $SH_{max}$  orientation about 8° more clockwise than data from focal mechanisms. This could be explained by the different distribution of the two data sets: the geological data cover mainly the High Andes of Peru and northern Bolivia where the Altiplano trends roughly in the NW-SE direction, whereas the focal mechanism data are not restricted to that region (Figure 5b). As mentioned above, the plateau-induced extensional stresses would be perpendicular to the NW-SE axis (north of 18°S) somewhat oblique to the E-W compression

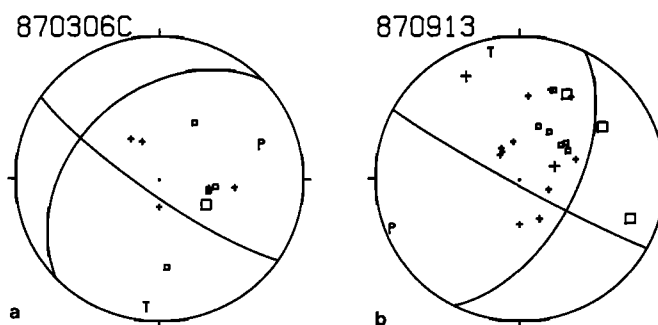


Fig. 4. Centroid-moment-tensor solutions (best double couple) inconsistent with polarity data as recorded by WWSSN and other South American stations. Crosses and squares are compressional and dilatational first motions; smaller symbols denote less reliable polarity data. (a) Event of March 6, 1987, 0814 UT, occurred in Colombia with  $m_b$  5.5; this was an aftershock of the main event with  $m_b$  6.5 at 0410 UT on the same day (event "870306B" in Figure 3). (b) Event of September 13, 1987, 2008 UT, occurred near the Chile-Argentina border with  $m_b$  5.8; the preferred focal mechanism solution is shown in Figure 2d.

related to the Nazca plate convergence. Superposition of these two sources of stress could result in an  $SH_{max}$  orientation in the High Andes with a slight tendency to be aligned along the axis of the Altiplano. Alternately, the  $8^\circ$  difference between the geological and focal mechanism data may be a result of local effects in the areas with high concentration of geological data such as in the Cuzco area of Peru (Figure 1).

In addition to the changes of stress orientations during Quaternary times, structural heterogeneities may be expected to cause some additional scatter in  $SH_{max}$  orientation. For example, beneath the high peaks of the eastern flank of Cordillera Blanca, in central Peru, the stress tensor determined with microearthquakes indicates a normal faulting regime with SW-NE extension [Deverchere *et al.*, 1989], whereas the major fault plane of the Cordillera Blanca shows N-S extension, consistent with the regional stress field, as indicated by the most recent fault striae [Sebrier *et al.*, 1988; Bonnot *et al.*, 1988]. Mercier *et al.* [this issue] suggested that the presence of a granitic batholith changes the stress field locally so that the focal mechanisms of the microearthquakes in or beneath the batholith are not representative of the regional field.

#### Regional Stress Field in Western South America

Scatter in  $SH_{max}$  orientation due to local heterogeneities needs to be averaged out to emphasize the direction of a more uniform, regional component. This was done in Figure 6a by taking the average orientation around grid points spaced every  $2.5^\circ$ . For each grid point all data within a search radius of  $2.5^\circ$  was used. Besides weighing the data according to the quality criteria (full weight for quality A, 0.7 for B, 0.35 for C, and 0.18 for D), linearly decreasing weight was assigned for distances between half and one search radius. The average orientation was calculated with the sum of the vectors with double angle [Davies, 1986]. The standard deviation of the orientations was then used to assign a quality to the grid point average. Most of the standard deviations (25 out of 31) were less than  $25^\circ$  (large bars in Figure 6a).

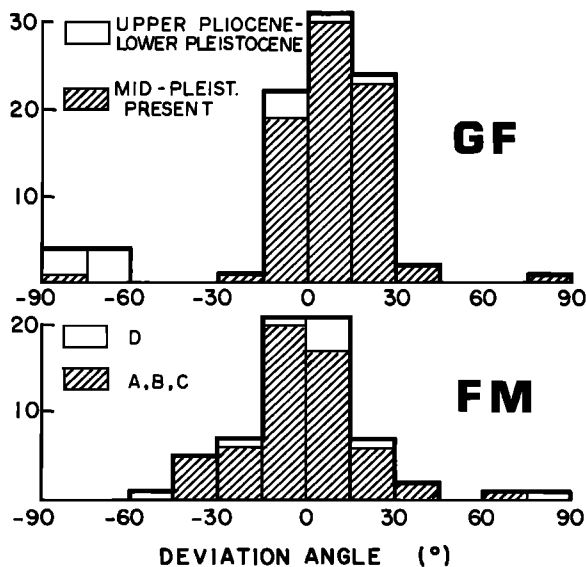


Fig. 5a. Distribution of the  $SH_{max}$  orientations in western South America with respect to the absolute plate motion [Minster and Jordan, 1978]. A positive angle means that the observed  $SH_{max}$  direction is oriented more clockwise with respect to the direction of absolute motion. Top histogram shows geological fault-slip data (GF); bottom histogram shows focal mechanism data (FM), with quality D data discriminated.

Figure 6 shows that the orientation of the "regional"  $SH_{max}$  (i.e., the grid point average) is remarkably constant in western South America. The change of strike of the Andean chain and the Peru-Chile trench (from roughly N-S south of  $18^\circ S$  to NW-SE north of  $18^\circ S$ ) apparently has no significant effect on the direction of the regional field. A comparison of the orientations of this regional field with the directions of relative motion between the Nazca and South American plates (calculated with the NUVEL1 pole of DeMets *et al.* [1990]) shows that the observed directions are about  $15^\circ$  more clockwise than the plate convergence direction (Figure 6b, histogram "N"). Taking into account the 95% confidence limit of the NUVEL1 pole that difference could vary between  $12^\circ$  and  $18^\circ$ . If the relative

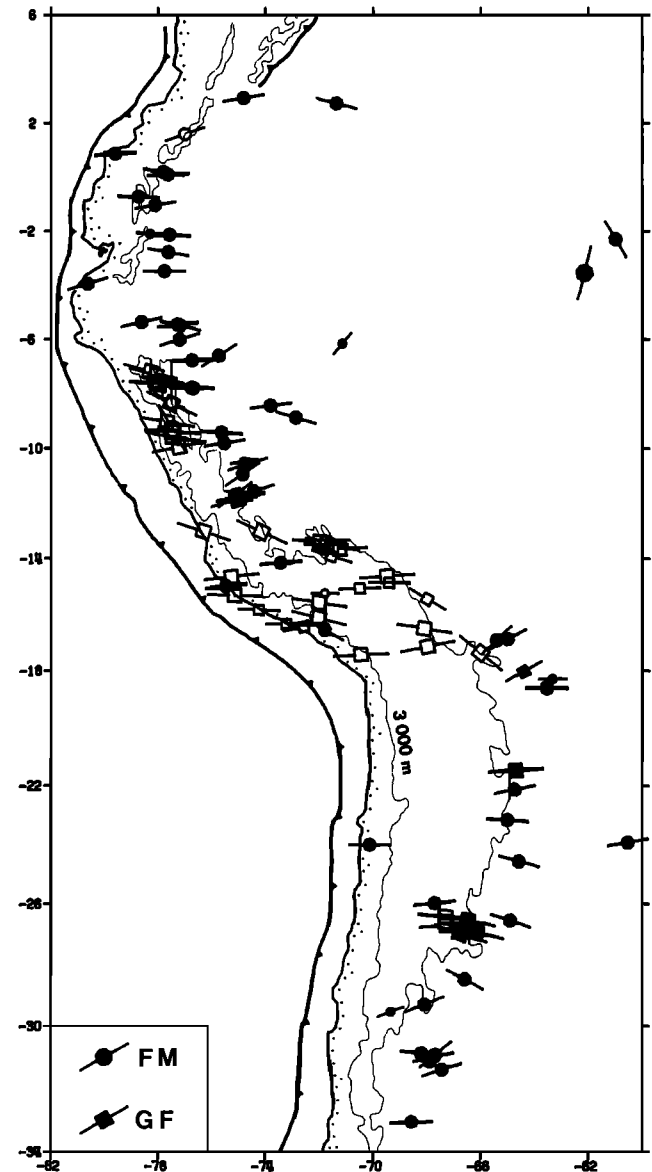


Fig. 5b.  $SH_{max}$  orientations for western South America. The contour line is the 3000 m elevation. Solid and open symbols denote compressional stresses (S1 horizontal) and normal stresses (S1 vertical); strike-slip earthquakes are indicated by solid circles as well. Circles and squares represent data from earthquake focal mechanisms (FM) and recent geological fault slip (GF), respectively. Only recent (Mid-Pleistocene to Present) geological data are shown. Large symbols represent data with qualities A and B; intermediate size quality C; small size quality D.



motion between Nazca and South America is taken only from the slip vectors of shallow thrust events in the subduction zone ("best fitting" pole of *DeMets et al.* [1990]), then the regional  $SH_{max}$  orientations are  $11^\circ$  more clockwise instead of  $15^\circ$ . So the consistent, clockwise difference between average  $SH_{max}$  directions and the Nazca-South America plate convergence is small but probably significant. If the observed regional field is compared with the absolute plate motion (using the AM1-2 poles of *Minster and Jordan* [1978] based on the hot spot frame), an average difference of only  $6^\circ \pm 11^\circ$  is found (Figure 6b, histogram "A"). This may be an indication that asthenospheric forces have an important contribution to the state of stress of the overlying plate. However, because of the large standard errors in the pole for absolute motion, the closer correlation of the regional  $SH_{max}$  with the absolute motion may not be significant. In fact, using the pole NUVEL1-HS2 for absolute motion, more recently determined by *Gripp and Gordon* [1990], a difference of  $13^\circ \pm 11^\circ$  is found.

Contour lines of the Wadati-Benioff zone (i.e., average hypocentral depths) in the subducting slab were compiled based primarily on the trend surfaces of *Bevis and Isacks* [1984] comple-

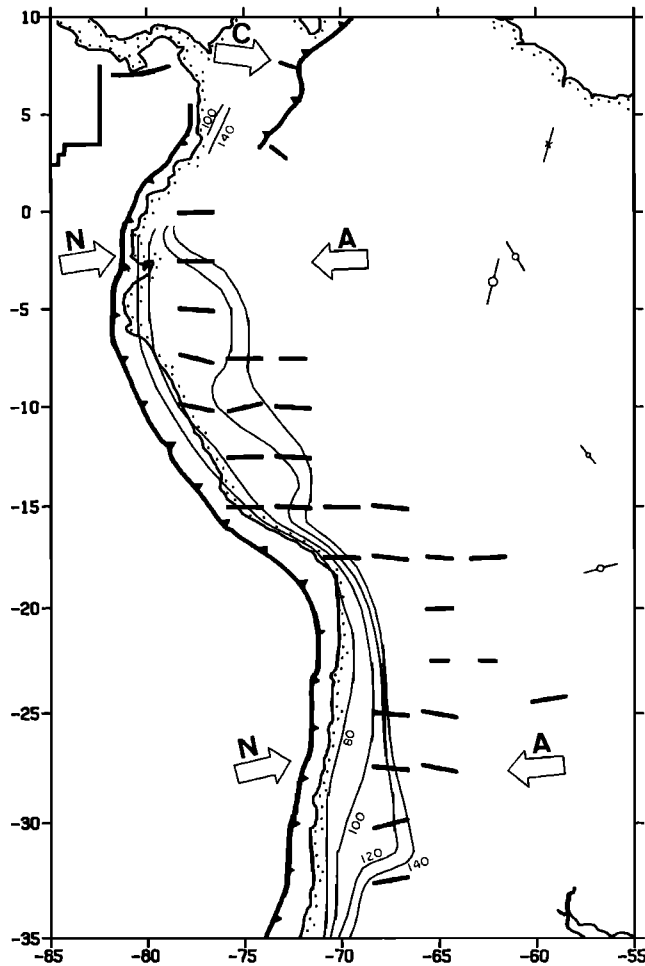


Fig. 6a. Regional  $SH_{max}$  orientations calculated as the average direction around grid points spaced  $2.5^\circ$  apart. Large and intermediate traces indicate standard deviations less than  $25^\circ$  and  $40^\circ$ , respectively. Small symbols correspond to standard deviations in the range  $40^\circ$ - $50^\circ$  (note that the value for a random distribution is  $52^\circ$ ). The Benioff zone is indicated by the 80- to 140-km isodepths. The "N" and "C" arrows indicate the directions of convergence of the Nazca and Caribbean plates [*DeMets et al.*, 1990]; the "A" arrows indicate the South America absolute motion [*Minster and Jordan*, 1978].

mented with more detailed data for Colombia [*Pennington*, 1981], southern Peru [*Grange et al.*, 1984; *Schneider and Sacks*, 1987], central Chile, and northwestern Argentina [*Smalley and Isacks*, 1987; *Pardo and Fuenzalida*, 1988]. The subducting plate is subhorizontal in northern and central Peru (from about  $3^\circ$ S to  $14^\circ$ S) and near the San Juan region of northwestern Argentina (from about  $28^\circ$ S to  $33^\circ$ S). If we consider that the hypocenters tend to occur, on average, about 10-20 km beneath the top of the subducting slab [*Smalley and Isacks*, 1987] and that the thickness of the overlying lithosphere should be about 100 km or more, we could expect that west of the 140 km depth contour, the South American plate is in contact with the underlying plate (or there is very little asthenospheric material in between). However, the orientation of the regional  $SH_{max}$  in areas of presumed plate contact does not appear to be significantly different from areas to the east where the South American plate directly overlies the asthenosphere (Figure 6b).

The E-W direction of the regional  $SH_{max}$  field in western South America is remarkably constant. It does not seem to be significantly affected by the change of strike of the Andes nor by the presence of a flat slab underneath. The difference between the observed orientations and the Nazca plate convergence direction is small but probably significant. This means that the Nazca plate "collision" does not seem to be the only direct contributor to the lithospheric stresses of the overlying South American plate. Besides plate boundary forces, lithospheric density heterogeneities can give rise to large tectonic stresses. *Fleitout and Froidevaux* [1982] showed that a heavy, cold lithospheric root can induce regional compressive stresses in the upper crust. Also, the downpull of the dipping, dense slab could produce compressional stresses in the upper lithosphere associated with downflexing of the upper plate [*Bott et al.*, 1989]. However, it is not clear how these other sources of stress would produce a regional field which is independent of the strike of the Andean plateau and the subducted slab. The state of stress in the lithosphere does not depend only on the forces acting at its nearest plate boundary but also on the balance of the forces acting on all its borders. Therefore, only numerical experiments [e.g., *Richardson et al.*, 1979; *Stefanick and Jurdy*, this issue; *Meijer and Wortel*, this issue] can show the combined effect of other forces such as ridge-push and asthenospheric shear stresses and help understand the origin of this uniform stress province in western South America.

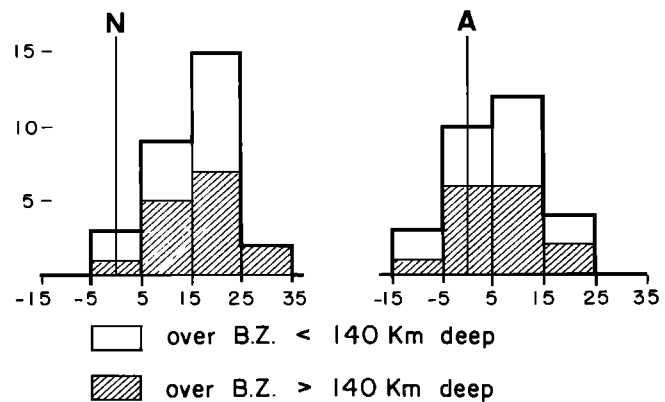


Fig. 6b. Distribution of the differences between the orientations of the regional  $SH_{max}$  (Figure 6a) and the directions of the Nazca-South America convergence (histogram "N") and the absolute plate motion (histogram "A"). Hatched data correspond to grid points above a Benioff zone deeper than 140 km.

STATE OF STRESS AND SEISMICITY  
IN MIDPLATE SOUTH AMERICA

Northern Amazonian Craton

With the presently available data it is not possible to determine the exact eastern limit of the E-W oriented  $SH_{max}$  province in western South America. At about 20°S this stress province may reach about half the continent (Figures 1 and 6a). At lower latitudes, two reverse fault earthquakes with N-S oriented  $P$  axes in the middle of the Amazonian basin and one break-out measurement in Guyana (Figures 1 and 7) suggest the existence of a different stress province in the north central part of the Amazonian craton. All epicenters for events with  $m_b$  greater than 3.5 are shown east of the dashed line in Figure 7. These seismicity data were taken from the catalog of *Berrocet et al.* [1984] covering up to 1982, complemented with the *Brazilian Seismic Bulletins* (1984-1990) up to 1989. The completeness threshold of this data set is about  $m_b$  4.5 since 1963 (from the worldwide network) and about  $m_b$  3.5 since 1980 with the regional seismic stations in the Amazonian region. The stress data showing N-S  $SH_{max}$  orientation are located within a cluster of epicenters which are separate from the sub-Andean seismicity and which may characterize a different seismicity/stress province in the Middle Amazonian basin and the central part of the Guyana shield. Figure 7 shows that between the sub-Andean E-W compressive stresses and the central Amazonian N-S compressive stress province there is a region of very low seismicity. This may indicate that the transition from the western South America stress province to the central Amazonian stress province occurs by a decrease of the stress magnitudes and not just a change of orientation.

The origin of these N-S stresses in the Amazonian craton is not known yet. Although the relative motion between the Caribbean and South American plates has a small N-S component [*DeMets et al.*, 1990] the Caribbean border seems to be too far (Figure 1) to be the main source of stress in the central Amazonian region. *Zoback* [this issue (a)] and *Richardson and Zoback* [1990] interpreted the compressive stresses perpendicular to the

axis of the Amazonian basin as due to loading effects of dense material intruded in the lower crust as evidenced by a chain of gravity highs (+40 to +90 mGal) along the axis of maximum thickness of the basin [*Nunn and Aires*, 1988]. The two reverse faulting events in the central part of the Amazon basin occurred at 23 and 45 km depth [*Assumpção and Suárez*, 1988]. Numerical modeling by *Richardson and Zoback* [1990] indicated maximum compressional deviatoric stresses, of the order of 100 MPa, at midcrustal depths, consistent with the observed depths of the two earthquakes.

Seismicity Around the Paraná Basin

Figure 8 shows all epicenters with magnitudes above  $m_b$  3.0 in and around the intracratonic Paleozoic Paraná basin. The seismicity data include historical and instrumental data from the same catalog used for Figure 7. Completeness thresholds are about  $m_b$  4.5 since 1963 (with the worldwide network) and about  $m_b$  3.0 since 1978 with the regional seismic stations in southeastern Brazil. The largest event in Figure 8 was  $m_b$  6.3 in 1955 (at 12.4°S, 57.3°W). The Paraná basin is characterized by very low seismicity. West of the basin the focal mechanisms are consistent with the E-W compressive stress province of western South America. North and east of the basin the available data are rather scattered to define any pattern in the stress field except to say that horizontal compression predominates. The focal mechanisms "f" and "g" refer to shallow (1-2 km) dam-induced activity. Quaternary fault slip data near the Atlantic coast have shown both extensional and compressional faulting; the extensional faulting being interpreted as relaxation of compressional cycles [*Riccomini et al.*, 1989]. If the scatter of the stresses east of the Paraná basin is not just a result of poor quality data, then local sources may predominate over plate wide forces.

It is not known why the interior of the Paraná basin is much less seismic than its borders. Gravity and isostatic studies in the northern part of the basin have indicated that lower crust densification (by upper mantle intrusions), rather than crustal

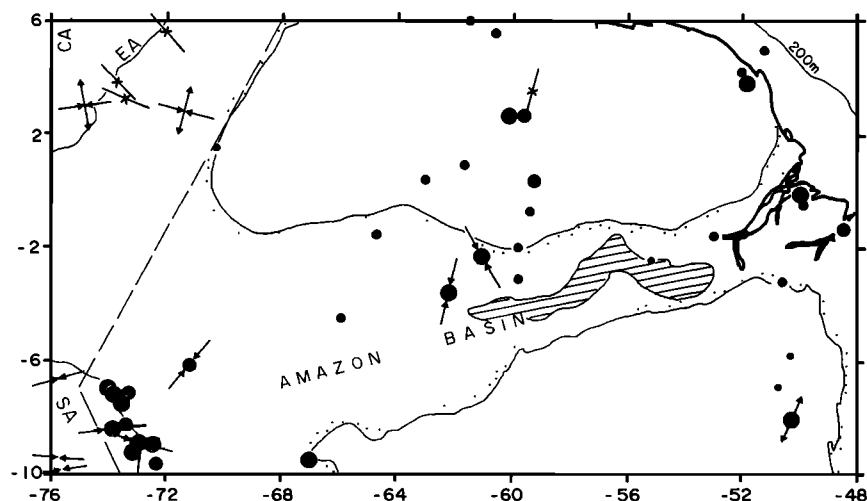


Fig. 7. Seismicity and stress data in the Amazonian region. Epicenters east of the dashed line cover the period 1950-1989. Symbol sizes denote magnitudes ranging from  $m_b$  3.5 to 5.5. Epicenters are complete for magnitudes above about  $m_b$  4.5 since 1963 and above  $m_b$  3.5 since 1980 (see text). West of the dashed line only stress directions are shown (same data points as in Figure 1). Convergent and divergent arrows are the  $P$  and  $T$  axes, respectively. For reverse (or normal) faulting earthquakes, only the  $P$  (or  $T$ ) axes are shown; for strike-slip events, both  $P$  and  $T$  are shown. The hatched area in the Middle Amazon basin represents positive Bouguer anomalies which roughly correspond to the location of lower crust dense material [*Nunn and Aires*, 1988]. SA is the sub-Andes of Peru; CA and EA are the central and eastern Cordilleras of Colombia.

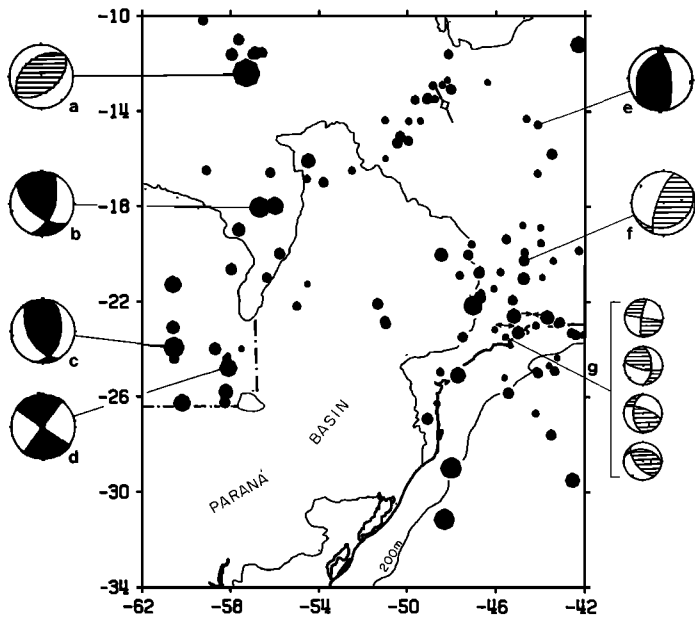


Fig. 8. Seismicity in and around the intracratonic Paleozoic Paraná basin. The dot-dashed lines indicate the Asunción arch and the West Pampean arch which separate the Paraná basin from the Chacos basin. Solid dots are historical and instrumental epicenters from 1861 to 1989 from the Brazilian catalog (Berrocal *et al.* [1984] and *Brazilian Seismic Bulletins*, 1984-1989). Symbol sizes denote magnitudes ranging from  $m_b$  3.0 to 6.3. Completeness thresholds are about  $m_b$  4.5 since 1963 and  $m_b$  3.0 since 1978. Focal mechanisms (lower hemisphere) have dark compressional quadrants for solutions with quality C and hatched for quality D. Divergent and convergent arrows east of the Paraná basin denote extensional and compressional stresses from Quaternary fault slip [Riccomini *et al.*, 1989]. The stress direction at about 14°S was obtained with hydraulic fracturing [Caproni and Armelin, 1990].

thinning, is a preferred model for the basin formation [Molina *et al.*, 1988]. However, free-air anomalies in the northern part of the basin are usually negative (average -20 mGal), indicating that the lower crustal densification does not compensate for the thickness of the low-density sediments. Thus, the resulting crustal mass deficit in the basin, as compared with neighboring areas, may cause extensional stresses in the upper crust [Fleitout and Froidevaux, 1982] which might balance the regional compressional stresses. The southern part of the Paraná basin, however, does not show negative free-air anomalies.

Whatever the cause of the aseismicity of the Paraná basin, it is interesting to note that the E-W compressional stress province of western South America seems to be limited here also by a region of low seismicity similarly to the Amazonian region.

#### Northeastern Brazil

Earthquakes in northeastern Brazil tend to occur around the Potiguar Mesozoic sedimentary basin (Figure 9) with focal depths usually less than 10 km [Assumpção *et al.*, 1989]. The maximum observed magnitude in this region was  $m_b$  5.2 (event b in Figure 9). Earthquakes in this region tend to occur in swarms lasting for many months or even years. The best documented series is the João Câmara earthquake sequence ("event" d in Figure 9) which started in August 1986, had two main events (November 30, 1986, and March 10, 1989, both with  $m_b$  5.0) and is still active with magnitudes up to  $m_b$  3.0 in 1991). The events of the João Câmara sequence define a 30-km-long rupture striking SW-NE with maximum depth of about 8-10 km [Ferreira *et al.*, 1987; Takeya *et al.*, 1989]. No surface rupture

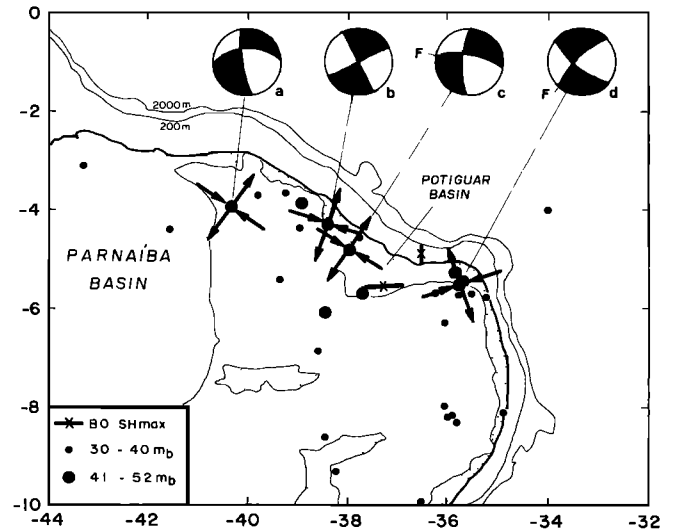


Fig. 9. Seismicity and focal mechanisms in northeastern Brazil. Historical and instrumental earthquake data (from 1808 to 1989) taken from the Brazilian catalog (as in Figures 7 and 8) are complete above  $m_b$  4.5 since 1963 and above  $m_b$  3.0 since about 1978. Maximum and minimum horizontal stresses as deduced from the earthquake focal mechanisms are indicated by convergent and divergent arrows: for solutions "a" and "b" they are the  $P$  and  $T$  axes; for solutions "c" and "d" (with identified fault plane, "F") they are plotted at 30° and 60° to the fault plane, instead of 45°. The continental shelf is shown by the 200-m and 2000-m bathymetry.

was found in the João Câmara area nor at any other epicentral area of northeastern Brazil. However, evidence of strong Holocene deformation has been inferred from tilted coastal peat deposits about 50 km northeast of the João Câmara epicentral area [Gusso and Bagnoli, 1989]. It should be noted that the seismicity observed in Figure 9 occurs mainly in areas of exposed Precambrian basement or at the edges of the Potiguar basin. No event greater than  $m_b$  4.0 has been observed south of 6°S, although no obvious difference is found in the Precambrian geological features north and south of this line. However, there seems to be a change of strike of structural trends within the Precambrian basement: north of 6°S the predominant trend is SW-NE, whereas to the south, E-W directions seem to prevail [Assumpção *et al.*, 1985, Figure 5].

Four focal mechanisms available for this area consistently show strike-slip motions with a small component of normal faulting (Figure 9). For two of these mechanisms, the fault plane could be clearly identified by the trend of hypocenters determined in microearthquake surveys (nodal plane "F" in Figure 9), and the  $SH_{max}$  estimate was taken at 30° to the fault plane. Only two breakout measurements (qualities C and D) are available in this region from boreholes in the Potiguar basin. The stress orientation inferred from breakouts in the offshore well was not well constrained (only 38 m total length). The five reliable estimates of  $SH_{max}$  in the Potiguar basin region (four focal mechanisms and the onshore breakout) have an average orientation of 102° (with standard deviation of 26°). The direction of the absolute plate motion in this part of the plate is 83° [Minster and Jordan, 1978] and the Mid-Atlantic ridge-push direction, using the NUVEL-1 rotation pole between Africa and South America [DeMets *et al.*, 1990], is 89°. Although only five measurements are not enough to define the regional stress field, it seems unlikely that the strike-slip motions observed in Figure 9 could be caused solely by either of those two plate-wide sources of stress (asthenospheric shear stresses and ridge-push)

especially taking into account that most focal mechanisms have a small component of normal motion.

The  $T$  axes (roughly equivalent to the least principal stress direction,  $S_3$ ) of the four earthquakes, and the  $Sh_{min}$  direction from breakouts in the onshore well, are all orthogonal to the northern coastline and continental margin, suggesting that the horizontal extensional component could be due to stresses generated by the continent-ocean structural transition. *Bott and Dean* [1972] have shown that the lateral variation in the density structure across continental margins can produce extensional stresses (30-40 MPa) perpendicular to the coastline on the continental side (and smaller compressional stresses on the oceanic side). The continental shelf in northeastern Brazil is very narrow (Figure 1), which may be an indication of a sharp continent-ocean transition. In addition, to lateral density variations, sediment loading at the continental shelf and continental rise coupled with subsidence of the cooling oceanic lithosphere also causes extensional stresses in the upper part of the continental crust. *Cloetingh et al.* [1984] modeled the flexure of a 100 Ma oceanic lithosphere due to a load of sediments with 8 km maximum thickness and obtained extensional stresses in the upper continental crust of about 270 MPa a few hundred kilometers from the edge of the continental shelf. If allowance is made for relaxation of stresses with faulting at the ocean-continent boundary during the evolution of the marginal basin, the extensional stresses in the upper continental crust may be smaller, about 100 MPa [*Turcotte et al.*, 1977], but still significant. Perhaps a superposition of these local extensional stresses with a regional E-W compression (either due to ridge-push or to asthenospheric drag) could produce the type of stresses which induce strike-slip motions (i.e.,  $S_1$  roughly parallel to the northern coast and  $S_3$  orthogonal to it). This simple model would also explain why the seismicity in northeastern Brazil is much reduced along the N-S trending coast (Figures 9 and 10): in this region the presumed E-W regional compression would be balanced by the local extension (also roughly E-W) due to lateral density contrasts and sediment loading at the continental shelf.

Some problems still need to be clarified for a better understanding of the seismicity in the Potiguar basin region. If this model of superposition of local and regional stresses is appropriate, seismicity should occur along the whole northern coast. The intracratonic Paleozoic Parnaíba basin (Figure 9), however, seems to be aseismic like the Paleozoic Paraná basin [*Assumpção*, 1989]. High heat flow values, greater than  $100 \text{ mW/m}^2$ , are commonly observed in northeastern Brazil, east of the Parnaíba basin [*Carneiro et al.*, 1989]. This high heat flow may indicate a reduced thickness of the brittle upper crust with a resulting concentration of stresses. The extensional stresses induced by lateral crustal density contrast [*Bott and Dean*, 1972] are an order of magnitude smaller than those predicted by sediment loading of an elastic lithosphere [*Cloetingh et al.*, 1984]. However, slow sedimentation rates on a viscoelastic lithosphere can reduce the flexural stresses by an order of magnitude [*Stein et al.*, 1989]. Flexure of the lithosphere due to sediment loading at the continental shelf and rise would also cause extensional stresses in the oceanic upper crust, but no significant seismicity has yet been detected offshore in northeastern Brazil (Figure 9). Probably, variations of the rheological properties of crustal materials [*Fleitout and Froidevaux*, 1982; *Stein et al.*, 1989] and the presence of weak zones in the upper crust [*Zoback*, this issue (b)] are also important.

*Zoback* [this issue (b)] showed that most intraplate earthquakes seem to occur in zones of weakness (preexisting faults) in response to the ambient crustal stresses. This would give support to the observation of *Assumpção et al.* [1985] that in the more seismic area (north of  $6^\circ\text{S}$ ) the structural trend is SW-NE, more favorable to rupturing, whereas in the aseismic area to the south the structural trend is oriented E-W, parallel to the presumed regional stress, inhibiting slipping. However, both in João Câmara (epicenter "d" in Figure 9 [*Takeya et al.*, 1989]) and in Palhano (epicenter "c" [*Assumpção et al.*, 1989]) the ruptures occurred in planes not related to any geological fault mapped at the surface, which indicates that more detailed studies are necessary to understand the relation between seismic "zones of weakness" and surface geological features.

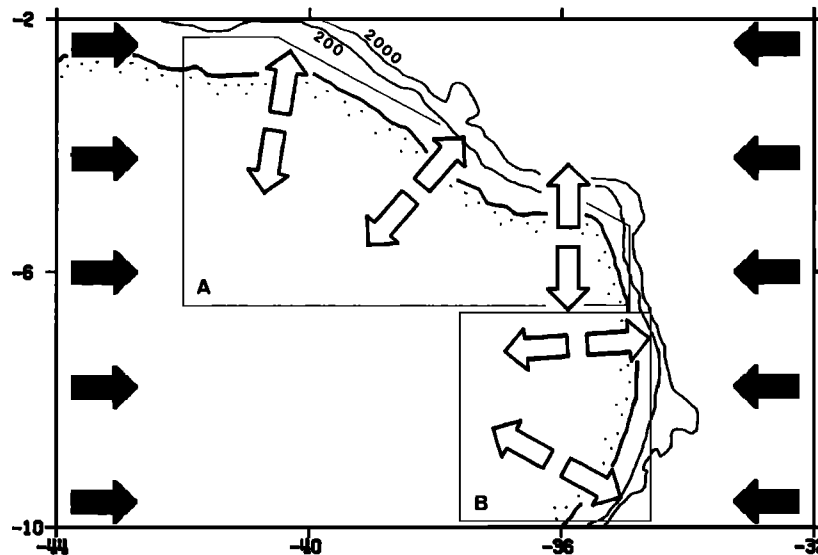


Fig. 10. Model of superposition of local and regional stresses in the upper crust. Open arrows denote local extensional stresses caused by lateral density contrasts and sediment loading at the continental margin. Solid arrows denote regional compressional stresses (possibly related to plate driving forces). Area "A", higher seismic activity with stresses inducing strike-slip faulting; area "B", lower seismic activity with local and regional stresses balancing each other.

## CONCLUSION

The compilation of stress data in South America, based mainly on focal mechanisms of intraplate earthquakes and geological fault slip data, is beginning to reveal the main characteristics of the regional stress field. Although large areas in South America remain devoid of data, the present data base should be helpful in constraining theoretical models of the plate driving forces.

In western South America, predominantly N-S extensional stresses in the High Andes ( $SH_{max}$  being the intermediate principal stress) and E-W compressional stresses in the sub-Andes ( $SH_{max}$  being the major principal stress) are now well established (see Mercier *et al.* [this issue] for a detailed description of Quaternary stresses in the Peruvian and Bolivian Andes). The orientation of the regional lithospheric  $SH_{max}$  field is remarkably constant and does not seem to be affected by the change of strike of the Andean chain nor by the presence of a flat slab underneath. The average difference between the regional  $SH_{max}$  orientation and the direction of the Nazca plate convergence is only about  $10^{\circ}$ - $15^{\circ}$  but seems to be significant. The closer alignment with the absolute plate motion direction, although statistically not significant, may indicate a substantial contribution of shear stresses from asthenosphere-lithosphere interactions east of the Andes. Alternatively, the coincidence of the regional  $SH_{max}$  direction with the absolute plate motion may be fortuitous with the regional field being the result of various plate boundary forces (and also gravitational body forces in a laterally varying lithosphere) which can only be modeled by numerical calculation [e.g., Richardson *et al.*, 1979; Fleitout and Froidevaux, 1982, 1983; Bott *et al.*, 1989; Stefanick and Jurdy, this issue]. At any rate, it seems unlikely that the Nazca plate "collision" should be the only major source of the regional stress field in western South America.

The eastern limit of the Andean E-W stress province seems to coincide with regions of very low seismicity, in the Amazonian craton and in the intracratonic Paraná basin. This may indicate that the Andean E-W stress field decreases in magnitude eastward and is replaced by stresses of different origin at the middle of the continent. More stress data in mid-plate South America, however, are necessary to substantiate this hypothesis.

In the central Amazonian region, the distribution of epicenters and the stress data suggest a different seismic and stress province characterized by roughly N-S compression. It is not clear yet whether this compressional field could result from the balance of the various plate boundary forces or could be due to local sources such as lower crustal loading as suggested by Richardson and Zoback [1990].

In northeastern Brazil, strike-slip focal mechanisms and the distribution of seismicity suggest a combination of plate-wide "regional" forces (such as asthenospheric drag or ridge-push) with local sources of stress (due to density contrasts across continental margins and sediment loading at the marginal basins). A similar combination of regional and local stresses was also observed in the Atlantic continental shelf of North America [Dart and Zoback, 1987; Zoback and Zoback, 1989].

Certainly, more stress data are necessary, especially east of the Andes, for a better definition of the stress provinces in mid-plate South America. Nevertheless, the data available so far should be a useful constraint to the various possible models of the forces that drive the plates.

*Acknowledgments.* I specially thank Mary Lou Zoback for continuous encouragement during the World Stress Map Project and many helpful discussions during the preparation of this paper. Data provided by INPRES, Argentina, and many other observatories is greatly appreciated. This work was supported by Brazilian grants CNPq 30.0227/79 and FAPESP 88/4163-8 and by an ICL travel grant.

## REFERENCES

- Allmendinger, R.W., M. Strecker, J.E. Eremchuk, and P. Francis, Neotectonic deformation of the southern Puna Plateau, NW Argentina, *J. S. Am. Earth Sci.*, **2**, 111-130, 1989.
- Anderson, H., Comparison of centroid-moment tensor and first motion solutions for western Mediterranean earthquakes, *Phys. Earth Planet. Inter.*, **52**, 1-7, 1988.
- Assumpção, M., Patterns of focal mechanism and seismic provinces in Brazil, *Proc. I Congr. Braz. Geophys. Soc.*, **1**, 467-472, 1989.
- Assumpção, M., and G. Suárez, Source mechanisms of moderate-size earthquakes and stress orientation in mid-plate South America, *Geophys. J.*, **92**, 253-267, 1988.
- Assumpção, M., G. Suárez, and J.A.V. Veloso, Fault plane solutions of intraplate earthquakes in Brazil: Some constraints on the regional stress field, *Tectonophysics*, **113**, 283-293, 1985.
- Assumpção, M., J.M. Ferreira, J.M. Carvalho, M.L. Blum, E.A. Menezes, D. Fontenele, and A. Aires, Seismic activity in Palhano, CE, October 1988, preliminary results, *Rev. Bras. Geofis.*, **7**, 11-17, 1989.
- Assumpção, M., J.A. Veloso, J.R. Barbosa, M. Blum, E. Neves, J. Carvalho, and A. Bassini, The earthquakes of Manga, MG, of March, 1990 (in Portuguese), *Proc. Braz. Geol. Congr. 36th*, **5**, 2154-2159, 1990.
- Bell, J.S., and D.I. Gough, Northeast-southwest compressive stress in Alberta: Evidence from oil wells, *Earth Planet. Sci. Lett.*, **45**, 475-482, 1979.
- Bellier, O., J. Macharé, and M. Sébrier, Extensión actual del nor Perú: estudio de la falla activa de Chaquibamba (norte del Departamento de la Libertad, Peru), *Bol. Soc. Geol. Perú*, **80**, 1-12, 1989.
- Berrocá, J., M. Assumpção, R. Antezana, C.M. Dias Neto, R. Ortega, and H. França, *Sismicidade do Brasil*, 320 pp., Instituto Astronômico e Geofísico, Universidade de São Paulo, Brazil, 1984.
- Bevis, M., and B.L. Isacks, Hypocentral trend surface analysis: Probing the geometry of Benioff zones, *J. Geophys. Res.*, **89**, 6153-6170, 1984.
- Bonnot, D., M. Sébrier, and J. Mercier, Evolution géodynamique Plio-Quaternaire du bassin intra-cordillerain du Callejon de Huaylas et de la région de la Cordillère Blanche, Pérou, *Geodynamique*, **3**, 57-83, 1988.
- Bott, M.H.P., and D.S. Dean, Stress systems at young continental margins, *Nature Phys. Sci.*, **235**, 23-25, 1972.
- Bott, M.H.P., G.D. Waghorn, and A. Whitaker, Plate boundary forces at subduction zones and trench-arc compression, *Tectonophysics*, **170**, 1-15, 1989.
- Cabrera, J., M. Sébrier, and J.L. Mercier, Active normal faulting in the high plateaus of central Andes: The Cuzco region (Peru), *Ann. Tectonicae*, **1**, 116-138, 1987.
- Caproni, N., Jr., and J.L. Armelin, Instrumentação das escavações subterrâneas da UHE Serra da Mesa, in *Simpósio sobre Instrumentação Geotécnica de Campo - SINGEO'90*, vol. 1, pp.249-257, Associação Brasileira de Geologia de Engenharia, São Paulo, 1990.
- Carey-Gailhardis, E., and J.L. Mercier, A numerical method for determining the state of stress using focal mechanisms of earthquake populations: Application to Tibetan teleseisms and microseismicity of Southern Peru, *Earth Planet. Sci. Lett.*, **82**, 165-179, 1987.
- Carneiro, C.D.R., V.M. Hamza, and F.F.M. Almeida, Ativação tectônica, fluxo geotérmico e sismicidade no nordeste oriental brasileiro, *Rev. Bras. Geoc.*, **19**, 310-322, 1989.
- Castillo, J.E., and J. Mojica, Orientaciones de esfuerzos actuales a partir de elongaciones tectónicas ("breakouts") en algunos pozos petroleros de los Llanos Orientales y del Valle Medio del Magdalena, Colombia, *Proc. I Congr. Braz. Geophys. Soc.*, **1**, 457-460, 1989.
- Chinn, D.S., and B.L. Isacks, Accurate source depths and focal mechanisms of shallow earthquakes in western South America and in the New Hebrides Island Arc, *Tectonics*, **2**, 529-563, 1983.

- Cipriani, J.C., In-situ stresses in the Caraiba underground mine (in Portuguese), *Rep. IPT-DIGEM 28170*, 168 pp., Inst. of Technol. Res., São Paulo, Brazil, 1990.
- Cloetingh, S.A.P.L., M.J.R. Wortel, and N.J. Vlaar, Passive margin evolution, initiation of subduction and the Wilson cycle, *Tectonophysics*, 109, 147-163, 1984.
- Cox, J.W., Long axis orientation in elongated boreholes and its correlation with rock stress data, *Trans. SPWLA Ann. Logging Symp.*, 24th, 1-14, 1983.
- Dart, R.L., and M.L. Zoback, Principal stress directions on the Atlantic continental shelf inferred from orientations of borehole elongations, *U.S. Geol. Surv. Open File Rep.* 87-283, 1987.
- Davies, J.C., *Statistics and Data Analysis in Geology*, 2nd ed., 646 pp., John Wiley, New York, 1986.
- DeMets, C., R.G. Gordon, D.F. Argus, and S. Stein, Current plate motions, *Geophys. J. Int.*, 101, 425-478, 1990.
- Departamento Nacional de Produção Mineral, Brasilia, Brazil, 1978.
- Deverchere, J., C. Dorbath, and L. Dorbath, Extension related to a high topography: Results from a microearthquake survey in the Andes of Peru and tectonic implications, *Geophys. J. Int.*, 98, 281-292, 1989.
- Dorbath, C., L. Dorbath, A. Cisternas, J. Deverchere, M. Diamant, L. Ocola, and M. Morales, On crustal seismicity of the Amazonian foothill of the central Peruvian Andes, *Geophys. Res. Lett.*, 13, 1023-1026, 1986.
- Doser, D.I., The Ancash, Peru, earthquake of November 10: Evidence for low angle normal faulting in the high Andes of northern Peru, *Geophys. J. R. Astron. Soc.*, 91, 57-71, 1987.
- Dziewonski, A.M., and J.H. Woodhouse, An experiment in systematic study of global seismicity: Centroid-moment tensor solutions for 201 moderate to large earthquakes of 1981, *J. Geophys. Res.*, 88, 3247-3271, 1983.
- Ferreira, J.M., M. Takeya, J.M. Costa, J.A. Moreira, M. Assumpção, J.A. Veloso, and R.G. Pearce, A continuing intraplate earthquake sequence near João Câmara, NE Brazil, preliminary results, *Geophys. Res. Lett.*, 14, 1042-1045, 1987.
- Ferreira, J.M., M. Takeya, E. Menezes, A. Ayres, and M. Assumpção, The Groiras, CE, earthquakes of March 31, 1988 (4.1 and 3.9 mb): Another example of strike-slip faulting in northeastern Brazil, paper presented at I Congress, Brazilian Geophys. Soc., Rio de Janeiro, Nov. 20-24, 1989.
- Fleitout, L., and C. Froidevaux, Tectonics and topography for a lithosphere containing density heterogeneities, *Tectonics*, 1, 21-56, 1982.
- Fleitout, L., and C. Froidevaux, Tectonic stresses in the lithosphere, *Tectonics*, 2, 315-324, 1983.
- Froidevaux, C., and Y. Ricard, Tectonic evolution of high plateaus, *Tectonophysics*, 134, 227-238, 1987.
- Grange, F., D. Hatzfeld, P. Cunningham, P. Molnar, S.W. Roecker, G. Suarez, A. Rodrigues, and L. Ocola, Tectonic implications of the microearthquake seismicity and fault plane solutions in southern Peru, *J. Geophys. Res.*, 89, 6139-6152, 1984.
- Gripp, A.E., and R.G. Gordon, Current plate velocities relative to the hot spots incorporating the NUVEL-1 global plate motion model, *Geophys. Res. Lett.*, 17, 1109-1112, 1990.
- Gusso, G.L.N., and E. Bagnoli, Evidências de intensa deformação tectônica em sedimentos costeiros holocênicos do Rio Grande do Norte, paper presented at I Congress, Brazilian Geophys. Soc., Rio de Janeiro, Nov. 20-24, 1989.
- Kadinsky-Cade, K., and R. Reilinger, Surface deformation associated with the November 23, 1977, Caucete, Argentina, earthquake sequence, *J. Geophys. Res.*, 90, 12,691-12,799, 1985.
- Kafka, A.L., and D.J. Weidner, Earthquake focal mechanisms and tectonic processes along the southern boundary of the Caribbean plate, *J. Geophys. Res.*, 86, 2877-2888, 1981.
- Katsui, Y., and R. Katz, Lateral fissure eruptions in the Southern Andes of Chile, *J. Fac. Sci. Hokkaido Univ., Ser. IV*, 13(4), 433-448, 1967.
- McKenzie, D.P., The relation between fault plane solutions for earthquakes and the directions of the principal stresses. *Bull. Seismol. Soc. Am.*, 59, 591-601, 1969.
- Meijer, P.T., and M.J.R. Wortel, The dynamics of motion of the South American plate, *J. Geophys. Res.*, this issue.
- Mendiguren, J.A., A procedure to resolve areas of different source mechanisms when using the method of composite nodal plane solution, *Bull. Seismol. Soc. Am.*, 70, 985-998, 1980.
- Mendiguren, J.A., and F.M. Richter, On the origin of compressional intraplate stresses in South America, *Phys. Earth Planet. Inter.*, 16, 318-326, 1978.
- Mercier, J.L., Extensional-compressional tectonics associated with the Aegean Arc: Comparison with the Andean Cordillera of south Peru-north Bolivia. *Philos. Trans. R. Soc. London, Ser. A*, 300, 337-355, 1981.
- Mercier, J.L., M. Sebrier, A. Lavenu, J. Cabrera, O. Bellier, J.-F. Dumont, and J. Macharé, Changes in the tectonic regime above a subduction zone of Andean type: The Andes of Peru and Bolivia during the Pliocene-Pleistocene, *J. Geophys. Res.*, this issue.
- Minster, J.B., and T.H. Jordan, Present-day plate motions, *J. Geophys. Res.*, 83, 5331-5354, 1978.
- Molina, E.C., N. Ussami, N.C. Sá, D. Blitzkow, and O.F. Miranda Filho, Deep crustal structure under the Parana basin (Brazil) from gravity studies, in *The Mesozoic Flood Volcanism of the Paraná Basin: Petrogenetic and Geophysical Aspects*, edited by E.M. Piccirillo, and A.J. Melfi, pp. 271-283, Instituto Astronômico e Geofísico, Universidade de São Paulo, São Paulo, 1988.
- Nunn, J.A., and J.R. Aires, Gravity anomalies and flexure of the lithosphere at the Middle Amazon Basin, Brazil, *J. Geophys. Res.*, 93, 415-428, 1988.
- Pardo, M., and A. Fuenzalida, Estructura cortical y subducción en Chile Central, in *Proceedings of V Congreso Geológico Chileno*, vol. II, pp. F247-F265, Sociedad Geológica de Chile, Santiago, 1988.
- Pennington, W.D., Subduction of the Eastern Panama Basin and seismotectonics of northwestern South America, *J. Geophys. Res.*, 86, 10,753-10,770, 1981.
- Plumb, R.A., and S.H. Hickman, Stress-induced borehole elongation: A comparison between the four arm dipmeter and the borehole in the Auburn geothermal well, *J. Geophys. Res.*, 90, 5513-5521, 1985.
- Raleigh, C.B., J.H. Healy, and J.D. Bredehoeft, Faulting and crustal stress at Rangely, Colorado, in *Flow and Fracture of Rocks*, *Geophys. Monogr. Ser.*, vol.16, edited by H.C. Heard et al., pp. 275-284, AGU, Washington, D.C., 1972.
- Riccomini, C., A.U.G. Peloggia, J.C.L. Saloni, M.W. Kohnke, and R.M. Figueira, Neotectonic activity in the Serra do Mar rift system (SE Brazil), *J. S. Am. Earth Sci.*, 2, 191-197, 1989.
- Richardson, R.M., and M.L. Zoback, Amazonas rift: Modeling stress around a paleozoic rift in South America (abstract), *Eos Trans. AGU*, 71, 1606, 1990.
- Richardson, R.M., S.C. Solomon, and N.H. Sleep, Tectonic stress in the plates, *Rev. Geophys.*, 17, 981-1019, 1979.
- Roa, H.M., The Upper Cenozoic volcanism in the Andes of Southern Chile (from 40.0 to 40.5 S.L.), in *Andean and Antarctic Volcanological Problems*, edited by O. Gonzales-Ferran, pp. 143-171, International Association of Volcanology and Chemistry of the Earth's Interior, Naples, Italy, 1976.
- Schneider, J.F., and I.S. Sacks, Stress in the contorted Nazca plate beneath southern Peru from local earthquakes, *J. Geophys. Res.*, 92, 13,887-13,902, 1987.
- Sébrier, M., J.L. Mercier, F. Megard, G. Laubacher, and E. Carey-Gailhardis, Quaternary normal and reverse faulting and the state of stress in the central Andes of Peru, *Tectonics*, 4, 739-780, 1985.
- Sébrier, M., J.L. Mercier, J. Macharé, D. Bonnot, J. Cabrera, and J.L. Blanc, The state of stress in an overriding plate situated above a flat slab: The Andes of central Peru, *Tectonics*, 7, 895-928, 1988.
- Sipkin, S.A., Estimation of earthquake source parameters by the inversion of waveform data: Global seismicity, 1981-1983, *Bull. Seismol. Soc. Am.*, 76, 1515-1541, 1986.
- Smalley, R.F., Jr., and B.L. Isacks, A high-resolution local network study of the Nazca plate Wadati-Benioff zone under western Argentina, *J. Geophys. Res.*, 92, 13,903-13,912, 1987.
- Sophia, C.M., and M. Assumpção, Padrão de ruptura da falha de Samambaia, RN, na reativação de fevereiro de 1987, *Proc. I Congr. Soc. Bras. Geofis.*, 1, 350-356, 1989.
- Stauder, W., Mechanism and spatial distribution of Chilean earthquakes with relation to subduction of the oceanic plate, *J. Geophys. Res.*, 78, 5033-5061, 1973.
- Stauder, W., Subduction of Nazca plate under Peru as evidenced by focal mechanisms and by seismicity, *J. Geophys. Res.*, 80, 1053-1064, 1975.
- Stefanick, M., and D.M. Jurdy, Stress observations and driving forces models for the South American plate, *J. Geophys. Res.*, this issue.
- Stein, S., S. Cloetingh, N.H. Sleep, and R. Wortel, Passive margin earthquakes, stresses and rheology, in *Earthquakes at North-Atlantic Passive Margins: Neotectonics and Postglacial Rebound*, edited by S. Gregersen and P.W. Basham, pp. 231-259, Kluwer Academic, Boston, Mass., 1989.
- Suárez, G., P. Molnar, and B. Burchfiel, Seismicity, fault plane solu-

- tions, depth of faulting, and active tectonics of the Andes of Peru, Ecuador, and southern Colombia, *J. Geophys. Res.*, *88*, 10,403-10,428, 1983.
- Takeya, M., J.M. Ferreira, R.G. Pearce, M. Assumpção, J.M. Costa, and C.M. Sophia, The 1986-1989 intraplate earthquake sequence near João Câmara, northeast Brazil — Evolution of activity, *Tectonophysics*, *167*, 117-131, 1989.
- Turcotte, D.L., J.L. Ahren, and J.M. Bird, The state of stress at continental margins, *Tectonophysics*, *42*, 1-28, 1977.
- Zoback, M.D., D. Moos, L. Mastin, and R.N. Anderson, Well bore breakouts and in situ stress, *J. Geophys. Res.*, *90*, 5523-5530, 1985.
- Zoback, M.L., First- and second-order patterns of stress in the lithosphere: The World Stress Map project, *J. Geophys. Res.*, this issue (a).
- Zoback, M.L., Stress field constraints on intraplate seismicity in eastern North America, *J. Geophys. Res.*, this issue (b).
- Zoback, M.L., and M.D. Zoback, State of stress in the conterminous United States, *J. Geophys. Res.*, *85*, 6113-6156, 1980.
- Zoback, M.L., and M.D. Zoback, Tectonic stress field of the continental United States, in Geophysical Framework of the Continental United States, edited by L. Pakiser and W. Mooney, *Mem. Geol. Soc. Am.*, *172*, 523-539, 1989.
- Zoback, M.L., et al., Global patterns of tectonic stress, *Nature*, *341*, 291-298, 1989.

— M. Assumpção, Depto. de Geofísica, IAG-USP, São Paulo, P.O. Box 9638, Brazil 01065.

(Received May 17, 1990;  
revised June 7, 1991;  
accepted June 16, 1991.)